Am J Physiol Renal Physiol 285: F1179–F1187, 2003.
First published September 2, 2003; 10.1152/ajprenal.00150.2003.

Dietary potassium restriction stimulates endocytosis of ROMK channel in rat cortical collecting duct

Po-Yin Chu,[1] Raymond Quigley,[2] Victor Babich,[1] and Chou-Long Huang[1]
[1]*Division of Nephrology, Department of Medicine, and* [2]*Department of Pediatrics, The University of Texas Southwestern Medical Center, Dallas, Texas 75390*

Submitted 17 April 2003; accepted in final form 27 August 2003

Chu, Po-Yin, Raymond Quigley, Victor Babich, and Chou-Long Huang. Dietary potassium restriction stimulates endocytosis of ROMK channel in rat cortical collecting duct. *Am J Physiol Renal Physiol* 285: F1179–F1187, 2003. First published September 2, 2003; 10.1152/ajprenal.00150.2003.—ROMK potassium channels are present in the cortical collecting ducts (CCDs) of the kidney and serve as the exit pathways for K^+ secretion in this nephron segment. Dietary K^+ restriction reduces the abundance of ROMK in the kidney. We have previously shown that ROMK undergoes endocytosis via clathrin-coated vesicles in *Xenopus laevis* oocytes and in cultured cells. Here, we examined the effect of dietary K^+ restriction on endocytosis of ROMK in CCDs using double-labeling immunofluorescent staining and confocal microscopic imaging in whole kidney sections as well as in individually isolated tubules. We found that ROMK abundance in kidney cortex and CCDs was reduced in rats fed a K^+-restricted diet compared with rats fed the control K^+ diet. In the control animals, ROMK staining was preferentially localized to the apical membrane of CCDs. Compared with control tubules, ROMK staining in CCDs was markedly shifted toward intracellular locations in animals fed a K^+-deficient diet for 48 h. Some of the intracellular distribution of ROMK colocalized with an early endosomal marker, early endosomal antigen-1 or with a late endosomal/lysosomal marker, lysosomal membrane glycoprotein-120. These results suggest that K^+ restriction reduces the abundance of ROMK in CCDs by increasing endocytosis and degradation of the channel protein. This decrease in the abundance of ROMK is likely important for maintaining K^+ homeostasis during K^+ deficiency.

early endosome antigen-1; lysosomal membrane glycoprotein-120; clathrin-coated vesicles; confocal imaging

THE LOW-CONDUCTANCE K^+ channels play important roles in K^+ secretion in the cortical collecting ducts (CCDs) and K^+ recycling in the thick ascending limb of Henle's loop (5, 23). Secretion of K^+ in CCDs is mediated by active transport of K^+ into the cell through the basolateral Na^+-K^+-ATPase and followed by passive movement of K^+ into the tubular fluid through the apical low-conductance K^+ channels.

Our understanding of renal K^+ channels was advanced by molecular cloning of cDNA for ROMK1 and its isoforms ROMK2 and ROMK3 (1, 6, 26). ROMK1 encodes a polypeptide of 391 amino acids. ROMK2 polypeptide lacks the first 19 amino acids of ROMK1 but is otherwise identical to ROMK1. ROMK3 polypeptide has a unique sequence for the first 19 amino acids in the NH_2 terminus. The remaining amino acids 20–399 of ROMK3 are identical to amino acids 13–391 of ROMK1. The distribution for the three ROMK isoforms varies and overlaps among tubular segments ranging from outer medullary thick ascending limb to inner medullary collecting ducts. Based on the distribution of mRNA and proteins and on biophysical characterization, it is believed that the low-conductance K^+ channels in the apical membranes of principal cells of the CCD are made up of heteromultimers of ROMK1 and ROMK2 (5).

As the final common pathway for K^+ secretion in CCDs, ROMK is an ideal target for regulation by variations in dietary K^+ intake. The density of active channels in the apical membrane of CCDs increases when dietary K^+ intake increases (4, 17, 18). This adaptation is important for maintaining K^+ homeostasis during high dietary K^+ intake (23). The increase in K^+ channel density during high dietary K^+ intake is not associated with an increase in the mRNA for ROMK in the renal cortex or isolated rat CCDs (4, 21). Several reports have suggested that the increase in channel density in K^+-adapted animals is due to a decrease in endocytosis and/or increase in exocytosis of the channel (13, 22).

Wald et al. (21) reported that a low dietary K^+ intake for 12 days decreases ROMK protein in both cortex and medulla of rat kidney. However, whether low K^+ intake decreases apical ROMK abundance in CCDs and the mechanism of the decrease in apical ROMK abundance are not known. We have recently shown that recombinant ROMK undergoes endocytosis via clathrin-coated vesicles in *Xenopus laevis* oocytes and in cultured Madin-Darby canine kidney cells (25). Nevertheless, it is unknown whether ROMK is present in endocytic vesicles in the kidney. The purpose of the present study was to investigate whether native ROMK in CCDs undergoes endocytosis and whether low K^+ intake stimulates endocytosis of ROMK in this nephron segment.

Address for reprint requests and other correspondence: C.-L. Huang, Dept. of Medicine, Univ. of Texas Southwestern Medical Ctr., 5323 Harry Hines Blvd., Dallas, TX 75390-8856 (E-mail: choulong.huang@utsouthwestern.edu).

The costs of publication of this article were defrayed in part by the payment of page charges. The article must therefore be hereby marked "*advertisement*" in accordance with 18 U.S.C. Section 1734 solely to indicate this fact.

Table 1. *Serum electrolytes from control and K^+-deficient rats*

	Na^+, meq/l	K^+, meq/l	Cl^-, meq/l	HCO_3, meq/l
Control K^+	139.3 ± 0.9	4.9 ± 0.5	105.1 ± 0.9	24.9 ± 0.8
K^+ deficient	138.8 ± 0.3	3.5 ± 0.2	96.8 ± 1.5	30.5 ± 1.3
Unpaired *t*-test	NS	$P < 0.03$	$P < 0.001$	$P < 0.01$

Values are means ± SE; $n = 6$ rats/group. NS, not significant.

METHODS

Experimental animals and diets. Male Sprague-Dawley rats (175–200 g) were used for this study. To study the effects of low dietary K^+ intake, rats were pair-fed either a K^+-deficient diet (no added K^+; TD95006, Harlan Teklad, Madison, WI) or a control K^+ diet (K^+ content 10 g/kg; TD88238) for 48 h. All animals were allowed to drink distilled water freely. Food intake and body weight were measured daily.

Preparation of whole kidney sections for immunostaining. Rats were anesthetized by intraperitoneal injection of thiopental (Pentothal; 100 mg/kg body wt) perfused retrograde through the abdominal aorta with a fixative consisting of 3% paraformaldehyde and 0.05% picric acid in a 6:4 mixture of cacodylate buffer (pH 7.4, containing 3 mM $MgCl_2$ and adjusted to 300 mosmol/kgH_2O with sucrose) and 10% hydroxyethyl starch in saline (HAES steril; Fresenius, Bad Homburg, Germany) (20). After 5 min of fixation, kidneys were perfused with the cacodylate buffer for an additional 5 min and embedded in cryoprotectant (OCT compound, Sakura Finetek, Torrance, CA) in standard biopsy molds (Cryomold, Miles, Elkhart, IN), sectioned (3 μm thick) at −22°C in the cryomicrotome, and frozen by submersion in liquid nitrogen.

Preparation of isolated CCDs for immunostaining. Rats were first sedated with Inactin (0.1 mg/100 g body wt) and then killed by decapitation. Blood was collected ($n = 6$ for both K^+-deficient and control groups) and centrifuged, and the serum was saved for electrolyte measurements. The kidneys were quickly removed and sliced into coronal slices. CCDs were dissected in cooled (4°C) modified Hanks' solution containing (in mM) 137 NaCl, 5 KCl, 0.8 $MgSO_4$, 0.33 Na_2HPO_4, 0.44 KH_2PO_4, 1 $MgCl_2$, 10 Tris·HCl, 0.25 $CaCl_2$, 2 glutamine, and 2 L-lactate. This solution was bubbled with 100% O_2 and had a pH of 7.4. Tubules were then transferred to a 1.2-ml thermostatically controlled bathing chamber and perfused with concentric glass pipettes. The perfusion solution simulated an ultrafiltrate of serum and contained (in

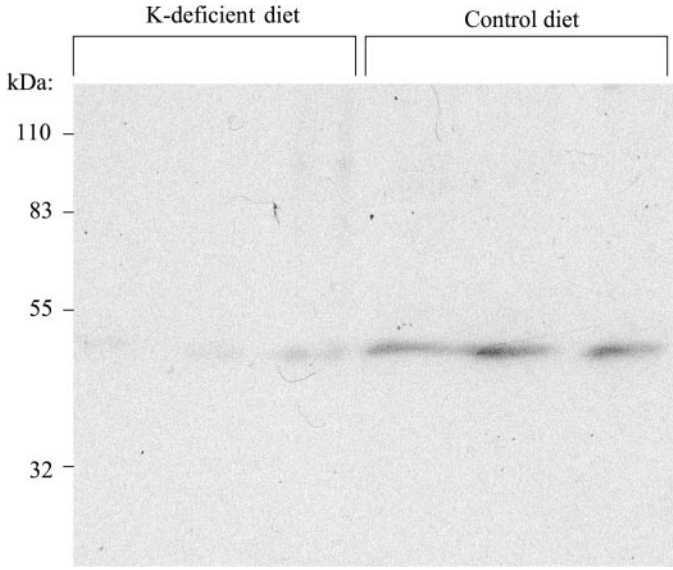

Fig. 1. Western blot analysis of abundance of ROMK in renal cortex from K^+-deficient (first 3 lanes) and control (last 3 lanes) animals. Animals were pair-fed either K^+- restricted or control diets for 48 h. Molecular weight markers (kDa) are shown on the *left*. Similar findings were observed in 2 different experiments. Each experiment includes 3 animals/group.

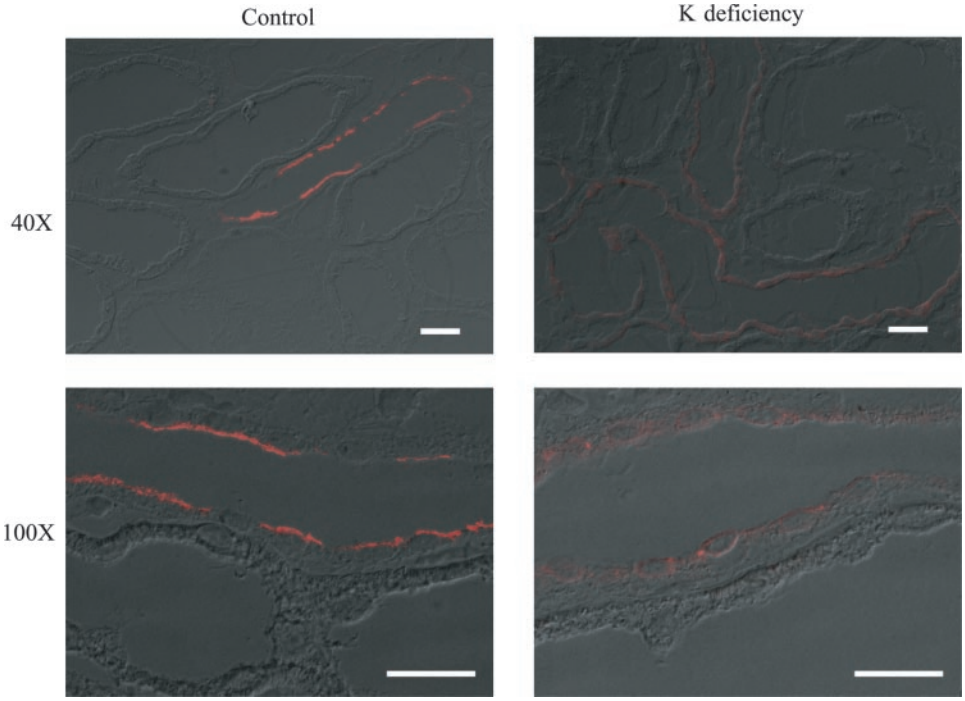

Fig. 2. Immunofluorescent staining of ROMK in renal cortex from K^+-deficient (*right*) and control (*left*) animals. Cortical sections from control and K^+-deficient animals were placed side by side in the same slide and stained with antibody against the COOH terminus of ROMK. Fluorescent and DIC images were obtained separately and then overlapped. Tubules in longitudinal sections are likely CCDs based on the morphology and mixtures of ROMK-positive (principal) cells and ROMK-negative (intercalated) cells. Microscopic images were obtained using ×40 or 100 objective lens (total magnification ×400 or 1,000). Images shown were enlargements of the actual microscopic images. The fold of enlargement can be calculated using the scale bar. Scale bars = 10 μm. Similar findings were observed in 15 different control and 15 different K^+-deficient animals.

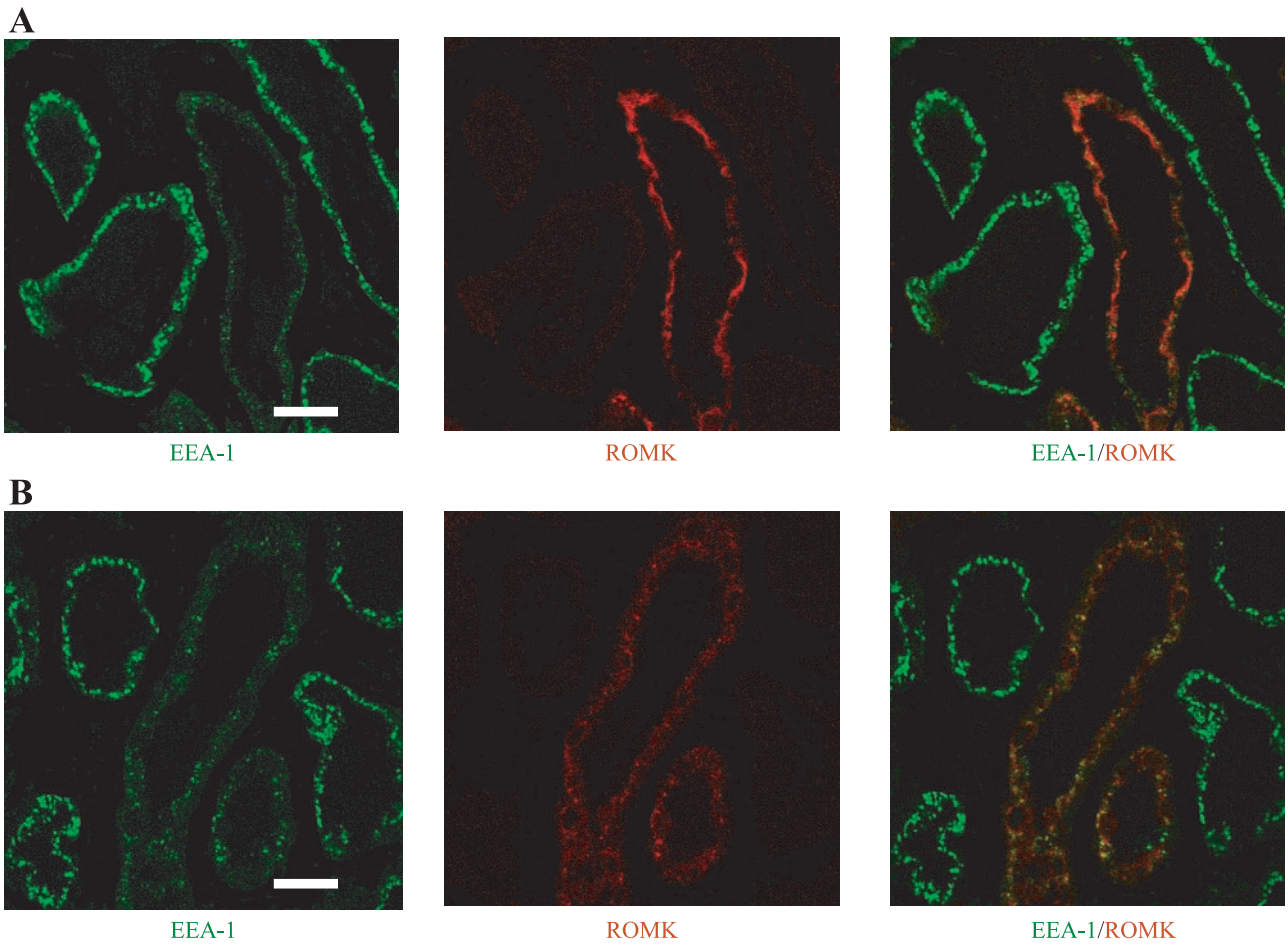

Fig. 3. Double-labeling immunofluorescent staining of ROMK and early endosome antigen-1 (EEA-1) in renal cortex from control (*A*) and K^+-deficient (*B*) animals. Sections from control and K^+-deficient animals were placed side by side in the same slide for staining by antibodies. Shown are images stained for EEA-1 (*left*, green) and for ROMK (*middle*, red). *Right*: merged images to indicate colocalization of ROMK and EEA-1 (yellow). Microscopic images were obtained using a ×40 objective lens (×400 magnification). Scale bars = 10 μm. Images shown are enlargements of the actual microscopic images. Similar findings were observed in 5 different control and 5 different K^+-deficient animals.

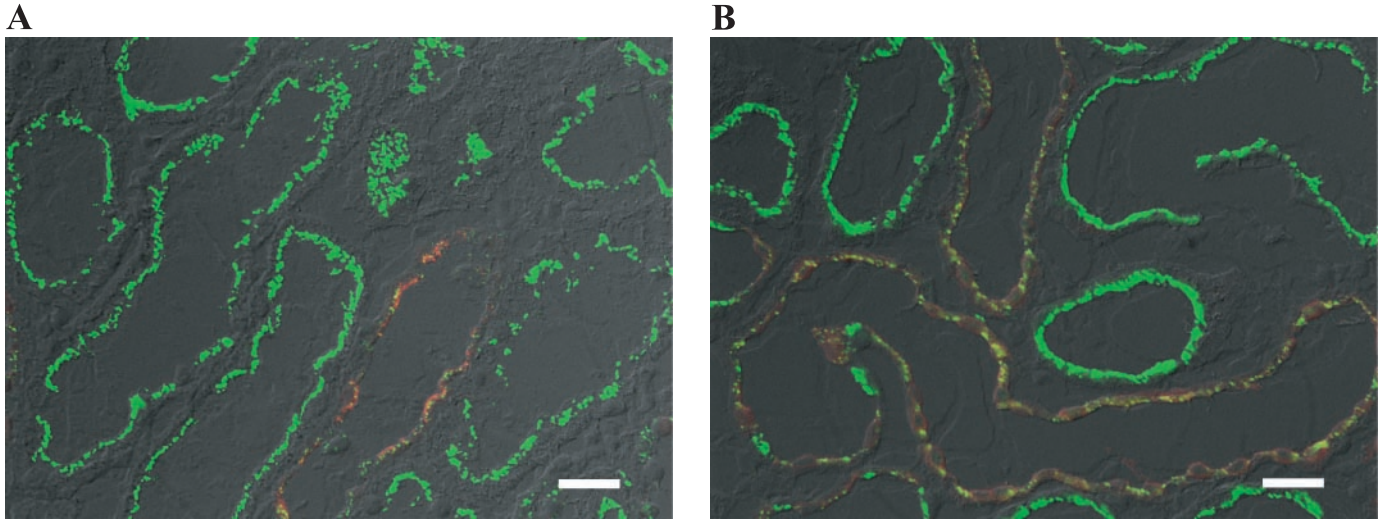

Fig. 4. Double-labeling immunofluorescent staining of ROMK and EEA-1 in renal cortex from control (*A*) and K^+-deficient (*B*) animals. Tissue sections and stainings were performed as in Fig. 3. Fluorescent images were overlapped with differential interference contrast (DIC) images to better illustrate subcellular distribution. Microscopic images were obtained using a ×40 objective lens (×400 magnification). Scale bars = 10 μm. Images shown are enlargements of the actual microscopic images. Similar findings were observed in 3 different control and 3 different K^+-deficient animals.

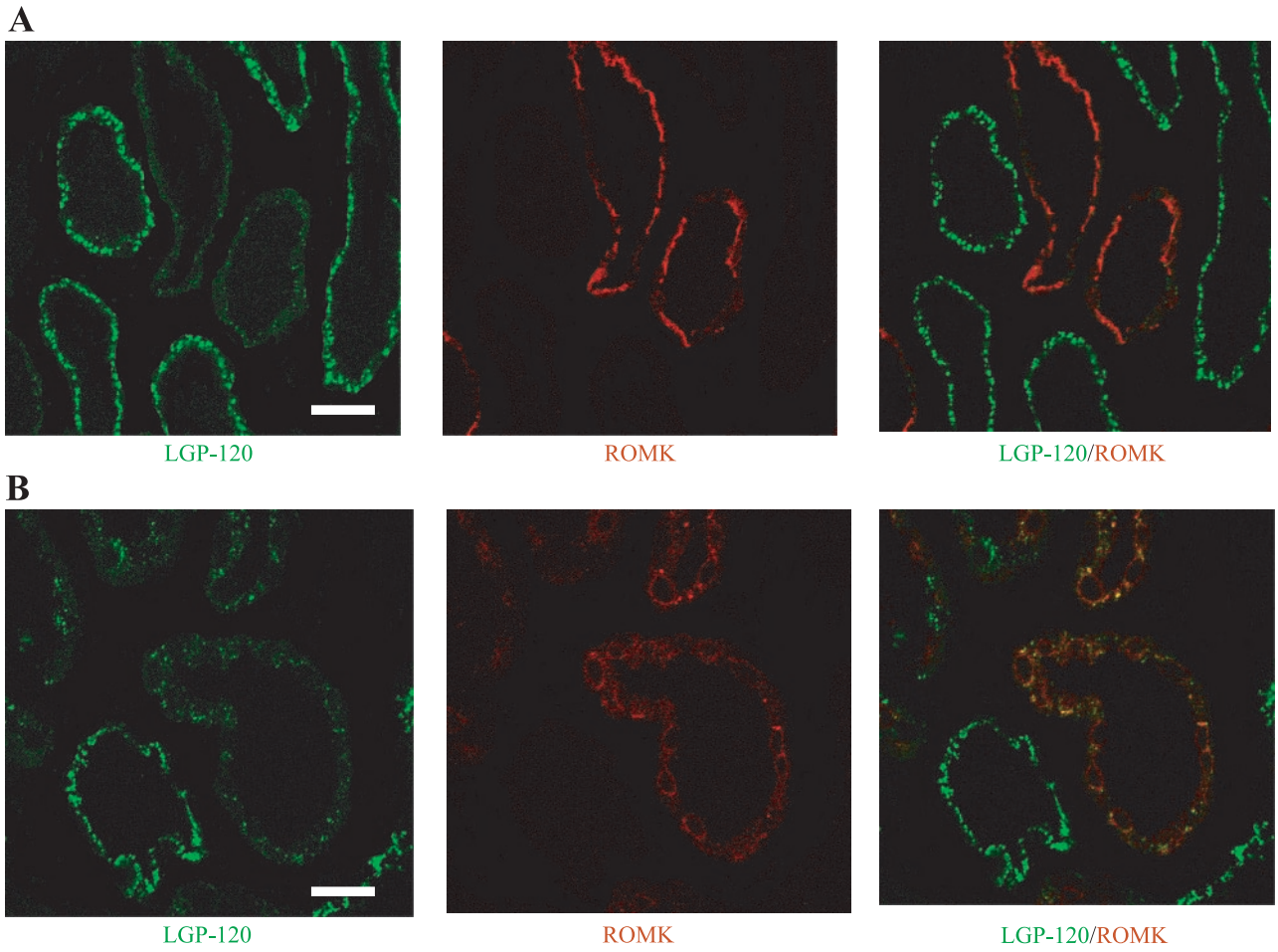

Fig. 5. Double-labeling immunofluorescent staining of ROMK and lysosomal glycoprotein-120 (LGP-120) in renal cortex from control (*A*) and K^+-deficient (*B*) animals. Sections from control and K^+-deficient animals were placed side by side in the same slide for staining by antibodies. Shown are images stained for LGP-120 (*left*, green) and for ROMK (*middle*, red). *Right*: merged images to indicate colocalization of ROMK and LGP-120. Microscopic images were obtained using a ×40 objective lens (×400 magnification). Scale bars = 10 μm. Images shown are enlargements of the actual microscopic images. Similar findings were observed in 5 different control and 5 different K^+-deficient animals.

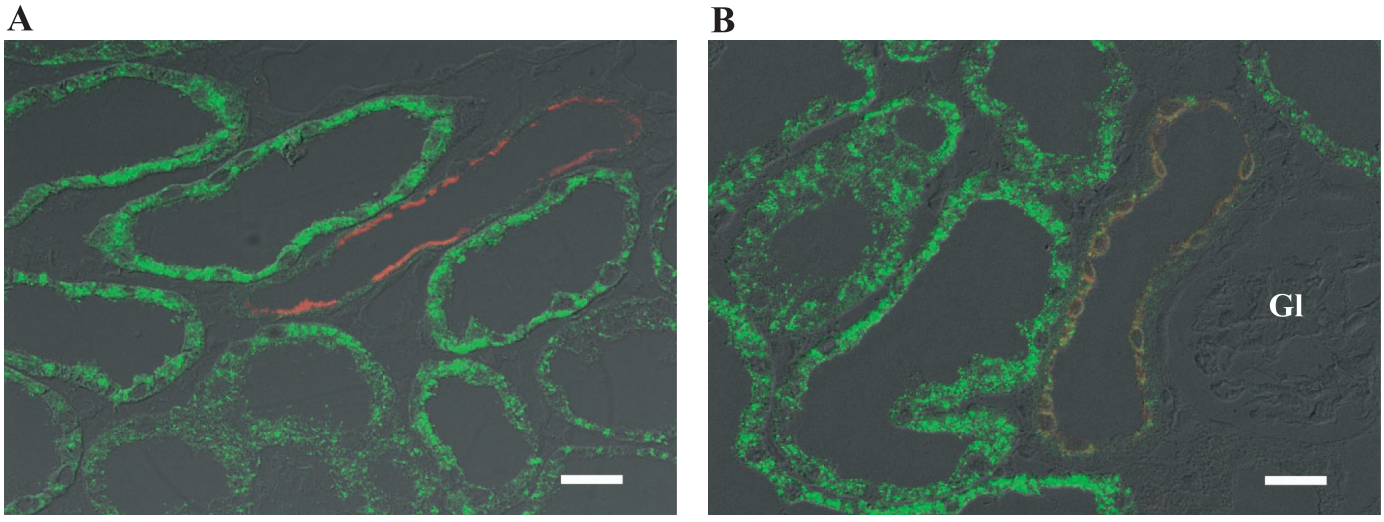

Fig. 6. Double-labeling immunofluorescent staining of ROMK and LGP-120 in renal cortex from control (*A*) and K^+-deficient (*B*) animals. Tissue sections and stainings were as in Fig. 5. Fluorescent images were overlapped with DIC images to better illustrate subcellular distribution. Microscopic images were obtained using a ×40 objective lens (×400 magnification). Scale bars = 10 μm. Images shown are enlargements of the actual microscopic images. Similar findings were observed in 2 different control and 2 different K^+-deficient animals.

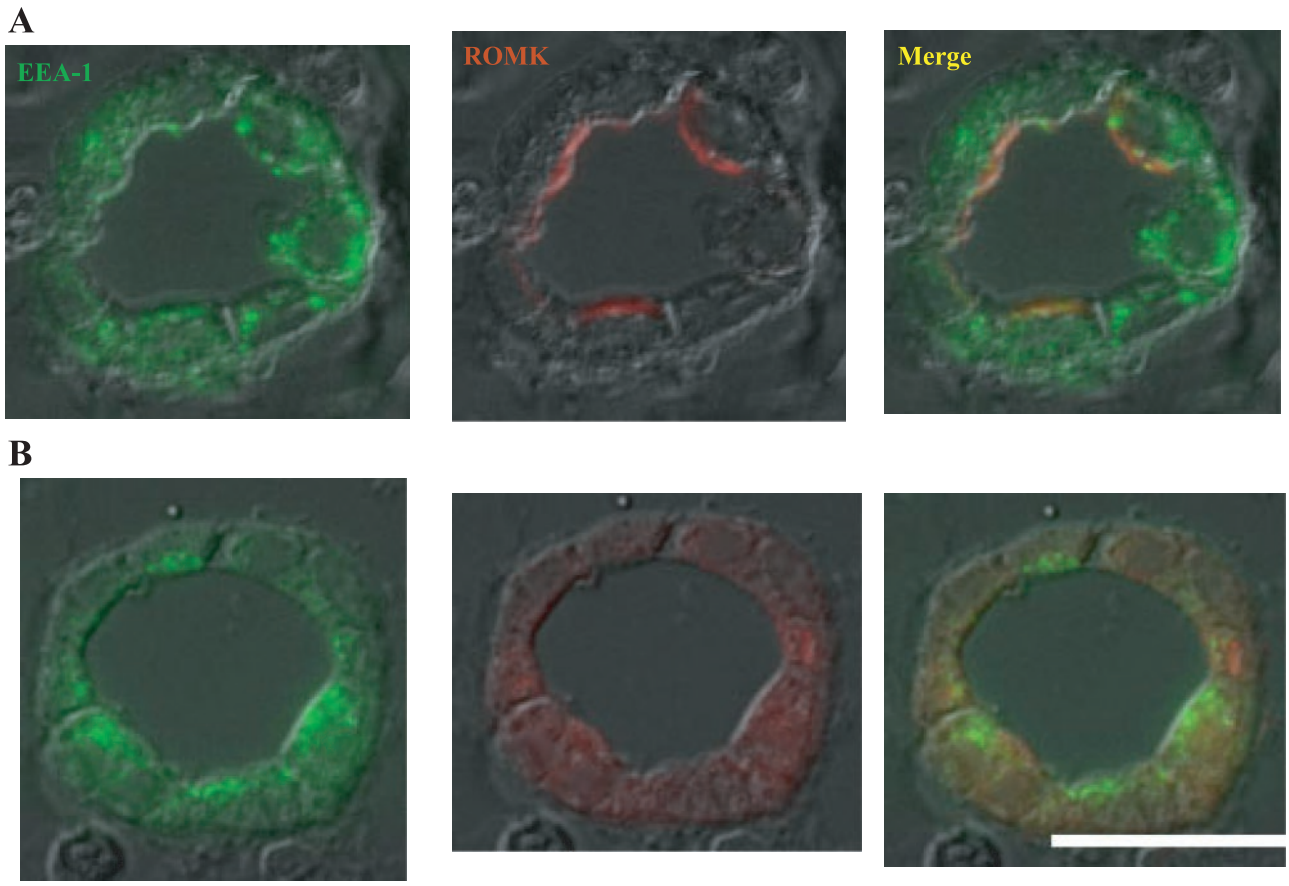

Fig. 7. Double-labeling immunofluorescent staining of ROMK and EEA-1 in individually isolated cortical collecting ducts (CCDs) from control (*A*) and K^+-deficient (*B*) animals. In these experiemtns, control and K^+-deficient tubules were placed in separate slides and stained by antibodies under the same condition. As in the cortical sections shown in Figs. 3–6, the staining for ROMK in CCDs was lower in the K^+-deficient animals (not shown). To allow comparison of merged images between control and K^+-deficient animals, the intensity of staining for ROMK and for EEA-1 was adjusted to be about equal (see METHODS). This upward adjustment of ROMK fluorescence increases the background in the K^+-deficient tubules (*B*, *middle*). The same tubules were stained for EEA-1 (*left*, green) and for ROMK (*middle*, red). Colocalization of ROMK with EEA-1 is shown in the merged images (*right*, yellow). Fluorescent images were overlapped with DIC images to better illustrate subcellular distribution. Microscopic images were obtained using a ×60 objective lens (×600 magnification). Scale bar = 10 μm. Images shown are enlargements of the actual microscopic images. Similar findings were observed in 8 different control and 6 different K^+-deficient tubules.

mM) 115 NaCl, 25 $NaHCO_3$, 5 KCl, 4 Na_2HPO_4, 1 $CaCl_2$, 1 $MgCl_2$, 5 glucose, and 5 alanine. The bathing solution was identical, except that it contained 6 g/dl of albumin. These solutions were bubbled with 95% O_2-5% CO_2 and had a pH of 7.4. Osmolalities of the perfusion and bathing solutions were adjusted to 295 mosmol/kgH_2O by the addition of water or NaCl. The bathing solution was exchanged at a rate of 0.5 ml/min to keep the osmolality and pH constant. Tubules were perfused for 20 min at 37°C, after which time the bath was changed to the fixative used in the whole kidney fixation (3% paraformaldehyde and 0.05% picric acid) and the tubule was allowed to fix while being perfused for another 20 min. The tubule was then transferred into a droplet of PBS with 10% gelatin warmed to 37°C. After the gelatin hardened, the tubule was then placed in the fixative for 24 h. This block was washed with PBS for 3 days and embedded in OCT cryoprotectant in biopsy molds. The molds were put in an aluminum foil (boat) floated on liquid nitrogen for rapid freezing. Thin sections (3 μm thick) were cut at −22°C in the cryomicrotome, mounted on slides coated with 0.1% poly-1-lysine (Sigma, St. Louis, MO), and stored at −20°C until use. Before use, sections were air-dried for 1 h at room temperature to ensure good adherence to the slide.

Double-labeling immunofluorescence staining and confocal imaging. For double-labeling of ROMK with early endosome antigen-1 (EEA-1) or with the lysosomal marker lysosomal membrane glycoprotein-120 (LGP-120), tissues were preincubated for 3 h at room temperature with 8% milk powder in PBS containing 1% Triton X-100. They were then incubated overnight at 4°C with an affinity-purified rabbit polyclonal antibody against the COOH terminus of ROMK (1:80 dilution in incubation buffer) (8) and with either a mouse monoclonal antibody against EEA-1 (1:10 dilution, BD Transduction Laboratories) or a mouse monoclonal antibody against rat lysosomal membrane glycoprotein LGP-120 (a gift from Dr. M. Levi, Univ. of Colorado Health Science Center at Denver) (1:10 dilution) (20). The sections were rinsed four times with PBS before incubation for 80 min at room temperature with the secondary antibodies. For double labeling of ROMK with EEA-1 (and LGP-120), the secondary antibodies (all from Jackson ImmunoResearch Laboratories, West Grove, PA) include Rhodamine red-X-conjugated donkey an-

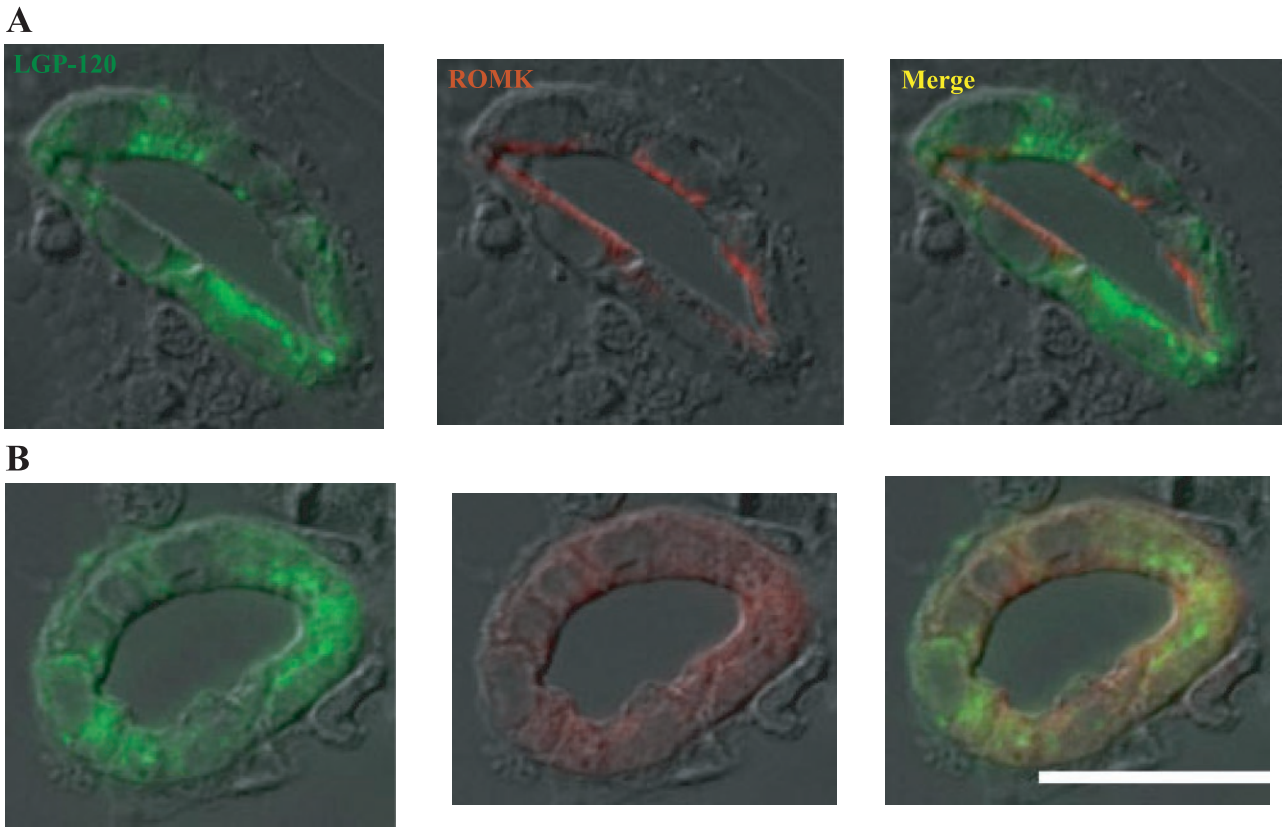

Fig. 8. Double-labeling immunofluorescent staining of ROMK and LGP-120 in individually isolated CCDs from control (*A*) and K^+-deficient (*B*) animals.The same tubules were stained for LGP-120 (*left*, green) and for ROMK (*middle*, red). Colocalization of ROMK with LGP-120 is shown in the merged images (*right*, yellow). Fluorescent images were overlapped with DIC images to better illustrate subcellular distribution. Microscopic images were obtained using a ×60 objective lens (×600 magnification). Scale bar = 10 μm. Images shown are enlargements of the actual microscopic images. Similar findings were observed in 5 different control and 6 different K^+-deficient tubules.

ti-rabbit IgG (1:500 dilution) and fluorescein-conjugated donkey anti-mouse IgG (1:500 dilution). After being rinsed with PBS, the sections were mounted using Vectashield mounting medium (Vector Laboratories, Burlingame, CA). Fluorescent images were visualized through a Zeiss ×40 or ×100 objective lens using a laser scanning confocal microscope (Zeiss LSM 410, Jana, Germany) (25). To detect the fluorescence of fluorescein, samples were excited at 488 nm and emissions were passed through a 510/560 band-pass filter. To detect fluorescence by Rhodamine red, samples were excited at 568 nm and emissions were passed through a 590 band-pass filter. Differential interference contrast (DIC) images were visualized using a Nikon inverted microscope (Eclipse TE 2000-U).

Western blot analysis. Kidney cortex from control and K^+-deficient rats (n = 3 each) were dissected immediately after death (8). Tissues were homogenized using a Teflon-glass homogenizer in an isolation buffer containing 250 mM sucrose, 30 mM HEPES (pH 7.4), and mixtures of protease inhibitors (Roche Applied Science, Indianapolis, IN). Membrane fractions (containing plasma and intracellular membranes) were pelleted by centrifugation at 120,000 *g* for 30 min and resuspended in the same buffer. Proteins were separated by 7.5% SDS-PAGE and transferred to nitrocellulose membranes. Western blot analysis was performed by incubating with rabbit anti-ROMK antibody (1:1,000 dilution) (8), followed by horseradish peroxidase-coupled donkey anti-rabbit secondary antibody (1:5,000 dilution) and visualized using enhanced chemiluminescence (Amersham Bioscience, Piscataway, NJ). Western blot analysis of β-actin was performed using monoclonal antibody against β-actin (Sigma-Aldrich).

RESULTS

We first examined the effect of dietary K^+ restriction on serum electrolytes. Serum K^+ concentration falls in response to dietary K^+ restriction (11). As shown in Table 1, the serum K^+ concentration decreased from 4.9 ± 0.5 to 3.5 ± 0.2 meq/l ($P < 0.03$) after 48 h of K^+ restriction. There was no difference in serum Na^+ concentration between the two groups. Serum HCO_3^- was higher in the K^+-restricted than the control animals (30.5 ± 1.3 vs. 24.9 ± 0.8 meq/l; $P < 0.001$). Thus our model of K^+ restriction for 48 h is sufficient to make the animals hypokalemic.

We next examined the effect of K^+ restriction on the abundance of ROMK in the rat kidney cortex. We focused on animals on a K^+-deficient diet for 48 h for the following reasons. First, the maximal effect of K^+ deficiency on ROMK abundance occurs at 48 h (11). Second, a longer duration of K^+ depletion (>72 h) may

cause hypertrophy of CCDs, especially the intercalated cells, which do not express ROMK (15). The abundance of ROMK was examined by immunoblot analysis using a previously characterized polyclonal antibody against the COOH terminus of ROMK (8). This antibody recognizes a common region of the three ROMK isoforms. A specific protein band consistent with the molecular size of ROMK (~45 kDa) was detected by the antibody in the cortex of control animals (Fig. 1, last 3 lanes). Compared with the control animals, abundance of ROMK in renal cortex was markedly reduced in animals fed a K^+-deficiency diet for 48 h (Fig. 1, 3 first 3 lanes). The abundance of β-actin was not different between control and K^+-deficient animals (not shown), suggesting a specific effect of K^+ deficiency on ROMK.

The effect of low K^+ intake on the abundance of ROMK was also examined using immunofluorescent staining. In the cortex, ROMK channels are present in thick ascending limb of Henle's loop, distal convoluted tubules, and CCDs (3, 8, 12, 24). Figure 2 shows overlapped images of immunofluorescent stainings of ROMK obtained using DIC microscopy in CCDs. ROMK stainings were also observed in other distal nephron segments besides CCDs (not shown). In the control animal (*left*), staining of ROMK was seen in a linear pattern consistent with preferential localization in and/or near the apical membranes. Staining for ROMK, however, was markedly reduced in the K^+-deficient animal. In addition, the distribution of ROMK became more diffuse and shifted toward intracellular sites (*right*).

The subcellular distribution of ROMK in CCDs in control and K^+-deficient animals was further examined using double-labeling immunofluorescent staining. After internalization, clathrin-coated vesiscles fuse to form early endosomes (10). Early endosomes, also named sorting endosomes, are pivotal in carrying endocytosed cargo molecules to either recycling vesicles or late endosomes and lysosomes for degradation (10). A unique resident protein of early endosomes, EEA-1, has been used as a specific marker of the organelle (14, 20). Double labeling using antibodies against ROMK and EEA-1 was performed to investigate whether ROMK undergoes endocytosis and whether K^+ deficiency affects endocytosis of ROMK. Figure 3 shows representative images of double labeling of ROMK and EEA-1 in control (Fig. 3*A*) and K^+-deficient (Fig. 3*B*) animals. Proximal tubules have very active endocytosis (20) and accordingly showed strong staining for EEA-1 [Fig. 3, *A* and *B*, *left* (green)]. Consistent with the idea that ROMK1 is absent in the proximal tubule, the strong EEA-1-positive tubules showed no stainings for ROMK [Fig. 3, *A* and *B*, middle (red) color]. Staining for ROMK was observed only in the distal nephron segments, which showed much weaker staining for EEA-1. As in Fig. 2 above, staining for ROMK showed a pattern of preferential distribution to the apical membrane in the control tubules (Fig. 3*A*, *middle*). The colocalization of ROMK1 with EEA-1 (yellow) was relatively low in control tubules (Fig. 3*A*, *right*). In contrast, tubules from K^+-deficient rats had decreased abundance of ROMK and shifted staining for ROMK toward intracellular locations (Fig. 3*B*, *middle*). The colocalization of ROMK with EEA-1 (yellow) was relatively more apparent in K^+ deficiency (Fig. 3*B*, *right*) compared with control (Fig. 3*A*, *right*). Nevertheless, the difference in colocalization of ROMK with EEA-1 between K^+-deficient and control animals is likely underestimated by these images due to a reduction of ROMK abundance in K^+ deficiency (see Fig. 7 for better contrast between K^+ deficiency and control when the intensity of ROMK staining is normalized). Figure 4 shows overlapped images of double labeling of ROMK and EEA-1 with images obtained by DIC microscopy in control (Fig. 4A) and K^+-deficient animals (Fig. 4*B*) to better illustrate subcellular distribution of colocalization of ROMK with EEA-1.

An increase in endocytosis of ROMK in K^+ deficiency may lead to an overall decrease in protein abundance if the endocytosed proteins are routed for degradation. We examined the effect of K^+ deficiency on degradation of ROMK after endocytosis by double labeling with LGP-120, a known marker for late endosomes and lysosomes (7, 9, 20). As shown, the colocalization of ROMK in the LGP-120-containing organelles was barely detectable in the control animals (Fig. 5*A*, *right*) and relatively more apparent in K^+ deficiency (Fig. 5*B*, *right*). Again, the colocalization of ROMK with LGP-120 in K^+ deficiency is likely underestimated due to a reduced abundance of ROMK (see Fig. 8 for a better comparison). Figure 6 shows overlapped images of double labeling of ROMK and LGP-120 with images obtained by DIC microscopy in control (Fig. 6*A*) and K^+-deficient animals (Fig. 6*B*) to better illustrate subcellular distribution of colocalization of ROMK with LGP-120.

To confirm that endocytosis and degradation of ROMK occur in CCDs, we used individually isolated CCDs for double-labeling immunofluorescent staining. In Figs. 3–6, the relative increase in the colocalization of ROMK with EEA-1 and LGP-120 in K^+-deficient vs control animals is likely underestimated due to a reduction of abundance of ROMK in K^+-deficient animals. Additionally, the relative weaker staining for EEA-1 and LGP-120 in CCDs compared with proximal tubules hampers the ability to investigate whether a low level of endocytosis occurs in the control tubules. To circumvent these problems, the images shown in Figs. 7 and 8 were obtained from individually isolated in vitro microperfused CCDs. The peak intensity of staining for ROMK and for EEA-1 or LGP-120 between control and K^+-deficient animals was adjusted to the same level. As shown in Fig. 7, stainings for EEA-1 in CCDs were widespread in intracellular sites (Fig. 7, *left*). Stainings for ROMK were concentrated in the region consistent with the apical membranes in control animal (Fig. 7*A*, *middle*) and became diffusely intracellular in K^+-deficient animals (Fig. 7*B*, middle). Merged images of staining for ROMK and for EEA-1 show slight colocalization of ROMK in EEA-1-containing endosomes in CCDs from control animals [Fig. 7*A*, *right* (yellow)]. This result suggests that there was a

low level of endocytosis occurring in the control tubule at baseline. Nevertheless, K^+ deficiency markedly increased the localization of ROMK in the EEA-1-positive endosomes in CCDs [Fig. 7*B*, *right* (yellow)]. Also, as shown in Fig. 6, a small amount of ROMK was present in the LGP-120-containing organelles in control animals (Fig. 8*A*). K^+ deficiency increased colocalization of ROMK in LGP-120-containing organelles (Fig. 8*B*).

DISCUSSION

Low dietary K^+ intake decreases abundance of ROMK in the kidney (11, 21). Wald et al. (21) reported that low K^+ intake for 12 days decreases mRNA for ROMK in kidney and medulla by ~50%, suggesting that downregulation of message may contribute to the decrease in ROMK protein in prolonged K^+ deficiency. On the other hand, Nakamura et al. (16) reported that K^+ deficiency for 2 days or longer upregulates message for ROMK1 in inner medulla. The authors of the latter study proposed that upregulation of ROMK1 in the inner medullary collecting duct will enhance K^+ recycling and contribute to increased secretion of NH_4^+ (and H^+) via H^+-K^+-ATPase in this segment (16). Wald et al. (21) also found that adrenalectomy decreases message for ROMK in the cortex but increases the message in medulla. Thus expression of ROMK may be differentially regulated in different tubular segments. CCDs makes up only a small fraction of ROMK-expressing tubules. Whether downregulation of message for ROMK contributes to the decrease in ROMK protein in CCDs in K^+ deficiency and, if so, the mechanism of the decrease are not known. In the present study, we find that low K^+ intake for 2 days decreases ROMK abundance and increases colocalization of ROMK in early endosomes and lysosomes in CCDs. These results suggest that increased endocytosis and degradation of the channel protein contribute to the decrease in ROMK channels in CCDs in K^+ deficiency. Nevertheless, it is possible that transcriptional regulation of message for ROMK may also contribute to the decrease in the density of the channel in CCDs, particularly during prolonged K^+ deficiency.

Serum K^+ concentration falls during low dietary K^+ intake (11). Conservation of K^+ is an essential adaptive mechanism for maintaining K^+ homeostasis in K^+ deficiency. One of the key adaptive mechanisms in K^+ deficiency is upregulation of H^+-K^+-ATPase in collecting ducts to enhance K^+ reabsorption (15, 19). Another potential mechanism is downregulation of ROMK in CCDs to decrease K^+ secretion. Patch-clamp studies examining the effects of K^+ deficiency on the density of K^+ channel in CCDs remain inconclusive. Some investigators reported that the density of K^+ channel in CCDs is lower in K^+-deficient rats compared with control rats (22), whereas others reported no detectable differences (18). Our results of increased endocytosis and degradation of ROMK in CCDs support the hypothesis that decrease in K^+ secretion via ROMK is also important for K^+ homeostasis during K^+ deficiency.

With the use of patch-clamp recording and inhibitors for endocytosis, several studies have provided evidence for endocytosis of ROMK in CCDs (13, 22). Our report of the use of individually isolated CCDs and double-labeling confocal immunofluorescent imaging provides the first immunological evidence in support of endocytosis of ROMK in this nephron segment. The signal(s) for stimulating endocytosis and degradation of ROMK by K^+ deficiency is not known. Potential signals include reduction in serum K^+ and/or aldosterone (15). Additionally, K^+-deficient animals have significant metabolic alkalosis, raising the possibility that alkalosis may contribute to increase in endocytosis in K^+ deficiency. The feasibility of immunostaining and imaging in individually isolated tubules provides an in vitro system for studying regulation of trafficking of ROMK by basolateral K^+ (and/or HCO_3^-) concentration and by aldosterone in the future.

The abundance of ROMK in cortex measured by Western blot analysis is reduced by K^+ restriction (Fig. 1). A similar reduction of cortical ROMK abundance by K^+ restriction has also been reported by Mennitt et al. (11). CCDs represent only a minor fraction of ROMK-expressing tubules in renal cortex. These results suggest that the abundance of ROMK is also reduced in other distal nephron segments. Mennitt et al. also found that K^+ restriction reduces the abundance of Na-K-2Cl cotransporter and suggested that reduction of ROMK and Na-K-2Cl cotransporter in the thick ascending limb of Henle's loop could be responsible for decreased reabsorption of NaCl observed in hypokalemia (11). Future study using double labeling of individually isolated thick ascending limb will also be useful in confirming the reduction of ROMK and examine the subcellular distribution in K^+ deficiency.

We thank Dr. Moshe Levi for providing anti-LGP-120 antibody and Dr. Michel Baum for support and encouragement.

DISCLOSURES

This work was supported in part by National Institute of Diabetes and Digestive and Kidney Diseases Grants (DK-54368 and DK-59530 to C.-L. Huang) and a grant-in-aid from the American Heart Assocation National Center (0150179N to C.-L. Huang).

REFERENCES

1. **Boim MA, Ho K, Shuck ME, Bienkowski MJ, Block JH, Slightom JL, Yang Y, Brenner BM, and Hebert SC.** ROMK inwardly rectifying ATP-sensitive K^+ channel. II. Cloning and distribution of alternative forms. *Am J Physiol Renal Fluid Electrolyte Physiol* 268: F1132–F1140, 1995.
2. **Casciola-Rosen LA, Renfrew CA, and Hubbard AL.** Luminal labeling of rat hepatocyte endocytic compartments. Distribution of several acid hydrolases and membrane receptors. *J Biol Chem* 267: 11856–11864, 1992.
3. **Ecelbarger CA, Kim GH, Knepper MA, Liu J, Tate M, Welling PA, and Wade JB.** Regulation of potassium channel Kir 1.1 (ROMK) abundance in the thick ascending limb of Henle's loop. *J Am Soc Nephrol* 12: 10–18, 2001.
4. **Frindt G, Zhou H, Sackin H, and Palmer LG.** Dissociation of K channel density and ROMK mRNA in rat cortical collecting tubule during K adaptation. *Am J Physiol Renal Physiol* 274: F525–F531, 1998.

5. **Hebert SC.** An ATP-regulated, inwardly rectifying potassium channel from rat kidney (ROMK). *Kidney Int* 48: 1010–1016, 1995.
6. **Ho K, Nichols CG, Lederer WJ, Lytton J J, Vassilev PM, Kanazirska MV, and Hebert SC.** Cloning and expression of an inwardly rectifying ATP-regulated potassium channel. *Nature* 362: 31–38, 1993.
7. **Howe CL, Granger BL, Hull M, Green SA, Gabel CA, Helenius A, and Mellman I.** Protein sequence, oligosaccharides, and membrane insertion of the 120-kDa lysosomal membrane glycoprotein (lgp120): identification of a highly conserved family of lysosomal membrane glycoproteins. *Proc Natl Acad Sci USA* 85: 7577–7581, 1988.
8. **Kohda Y, Ding W, Phan E, Housini I, Wang J, Star RA, and Huang CL.** Localization of the ROMK potassium channel to the apical membrane of distal nephron in rat kidney. *Kidney Int* 54: 1214–1223, 1998.
9. **Malide D and Cushman SW.** Morphological effects of wortmannin on the endosomal system and GLUT4-containing compartments in rat adipose cells. *J Cell Sci* 110: 2795–2806, 1997.
10. **Mellman I.** Endocytosis and molecular sorting. *Annu Rev Cell Biol* 12: 575–625, 1996.
11. **Mennitt PA, Frindt G, Silver RB, and Palmer LG.** Potassium restriction downregulates ROMK expression in rat kidney. *Am J Physiol Renal Physiol* 278: F916–F924, 2000.
12. **Mennitt PA, Wade JB, Ecelbarger CA, Palmer LG, and Frindt G.** Localization of ROMK channels in the rat kidney. *J Am Soc Nephrol* 8: 1823–1830, 1997.
13. **Moral Z, Dong K, Wei Y, Sterling H, H, Deng Ali S, Gu R, Huang XY, Hebert SC, Giebisch G, and Wang WH.** Regulation of ROMK1 channels by protein-tyrosine kinase and -tyrosine phosphatase. *J Biol Chem* 276: 7156–7163, 2001.
14. **Mu FT, Callaghan JM, Steele-Mortimer O, Stenmark H, Parton RG, Campbell PL, McCluskey J, Yeo JP, Tock EP, and Toh BH.** EEA1, an early endosome-associated protein. EEA1 is a conserved alpha-helical peripheral membrane protein flanked by cysteine "fingers" and contains a calmodulin-binding IQ motif. *J Biol Chem* 270: 13503–13511, 1995.
15. **Muto S.** Potassium transport in the mammalian collecting duct. *Physiol Rev* 81: 85–116, 2001.
16. **Nakamura S, Amlal H, Galla JH, and Soleimani M.** NH_4^+ secretion in inner medullary collecting duct in potassium deprivation: role of colonic H^+-K^+-ATPase. *Kidney Int* 56: 2160–2167, 1999.
17. **Palmer LG, Antonian L, and Frindt G.** Regulation of apical K and Na channels and Na/K pumps in rat cortical collecting tubule by dietary K. *J Gen Physiol* 104: 693–710, 1994.
18. **Palmer LG and Frindt G.** Regulation of apical K channels in rat cortical collecting tubule during changes in dietary K intake. *Am J Physiol Renal Physiol* 277: F805–F812, 1999.
19. **Silver RB and Soleimani M.** H^+-K^+-ATPase: regulation and role in pathophysiological states. *Am J Physiol Renal Physiol* 276: F799–F811, 1999.
20. **Sorribas V, Halaihel N, Alcalde A, Morales RM, Sarasa M, Zajicek HK, Wang H, Rogers T, Puttaparthi K, Cronin RE, and Levi M.** Gentamicin causes endocytosis of Na/Pi cotransporter protein (NaPi-2). *Kidney Int* 59: 1024–1036, 2001.
21. **Wald H, Garty H, Palmer LG, and Popovtzer MM.** Differential regulation of ROMK expression in kidney cortex and medulla by aldosterone and potassium. *Am J Physiol Renal Physiol* 275: F239–F245, 1998.
22. **Wang W-H, Lerea KM, Chan M, and Giebisch G.** Protein tyrosine kinase regulates the number of renal secretory channels. *Am J Physiol Renal Physiol* 278: F165–F172, 2000.
23. **Wright FS and Giebisch G.** Regulation of potassium excretion. In: *The Kidney: Physiology and Pathophysiology* (2nd ed.), edited by Seldin DW and Giebisch G. New York: Lippincott Williams & Wilkins, 1992, p. 2209–2246.
24. **Xu JZ, Hall AE, Peterson LN, Bienkowski MJ, Eessalu TE, and Hebert SC.** Localization of the ROMK protein on apical membranes of rat kidney nephron segments. *Am J Physiol Renal Physiol* 273: F739–F748, 1997.
25. **Zeng WZ, Babich V, Ortega B, Quigley R, White SJ, Welling PA, and Huang CL.** Evidence for endocytosis of ROMK potassium channel via clathrin-coated vesicles. *Am J Physiol Renal Physiol* 283: F630–F639, 2002.
26. **Zhou H, Tate SS, and Palmer LG.** Primary structure and functional properties of an epithelial K^+ channel. *Am J Physiol Cell Physiol* 266: C809–C824, 1994.